2011 50th IEEE Conference on Decision and Control and
European Control Conference (CDC-ECC)
Orlando, FL, USA, December 12-15, 2011

Model Predictive Control of Remotely Operated Underwater Vehicles

A. Molero, R. Dunia, J. Cappelletto and G. Fernandez

Abstract— **This paper describes the implementation of a model predictive controller novel in an underwater robot vehicle. This work also shows the development of an underwater vehicle model that accounts for physical, hydrodynamic and restorative effects, while the damping coefficients are neglected in the prediction of the vehicle position and orientation. The vehicle kinematic and dynamic models are linearized and arranged into the state space form inside the predictive controller. The model helps to determine the future position and orientation of the vehicle to track a predefined underwater trajectory in an optimal way. The results show that the predictive controller offered significant benefits compared to PID controllers by reducing the MSE and RMS by 40% and 76% respectively.**

I. INTRODUCTION

A Remote Operated Vehicle (ROV) is a type of Unmanned Underwater Vehicle (UUV) connected to the surface through a cable or umbilical line. ROVs can perform important underwater tasks that include assisting the offshore exploration and production of oil and gas [1] and studying marine life and collecting deep water samples [2]. Improving ROVs involves not only researching their design, but also the reliability of their operation and maneuverability [3].

The design, implementation and testing of the guidance and control systems for ROVs have been addressed by several researchers during the last decade [4],[5]. The design of robust tracking controllers using proportional and derivative action with nonlinear compensation has proved to be stable, converging the tracking error exponentially [6]. Model-based closed loop trajectory tracking control has been successfully deployed in several ROVs in the United States and the United Kingdom [7]. Soylu, Buckham and Podhorodesky have proposed the use of Chattering-free sliding mode and l_∞ controllers for the trajectory control of ROVs to incorporate the thruster saturation limits as part of the controller design [8].

The control techniques mentioned above have significantly improved the operation reliability and task accuracy of ROVs [5]. Nevertheless, these control algorithms do not consider the effect of forecast perturbation and out-coming tracking maneuvers that can be well predicted by a dynamic model. Model Predictive Control (MPC) [9], [10] is a model-based control algorithm that solves a finite horizon optimal control problem, using the current state of the system as the initial state. The optimization results in a sequence of optimal control actions where only the first control move is implemented [11].

This paper demonstrates the development of a ROV nonlinear model and its use to apply MPC. Such a novel application requires the use of reliable and fast real time optimization algorithms inside the controller [12]. PoseiBoT, the vehicle prototype depicted in figure 1, is used in this application. It represents a second generation of ROVs developed for multivariable control applications.

Fig. 1. Remotely Operated Underwater Vehicle, PoseiBoT.

In MPC the accuracy of the ROV translation, speed and trajectory tracking depends of the quality of the model. The model presented and used in this work considers: physical features (inertia and Coriolis), hydrodynamic effects (added mass) and restorative forces (gravity and buoyancy).The inertia tensor and center of gravity of PoseiBoT were determined using 3D CAD software. PoseiBoT was approximated to a prolate ellipsoid [15] to calculate the added mass terms. Finally the damping effect is negligible for the ROV speed range considered in this work [15]. A linearized state space model was used in the implementation of MPC.

Predictive control with conditional penalties [12] in the cost function is implemented to manage the position and orientation of PoseiBoT. The performance of the controller is determined by using the control signal (RMS) and the tracking error (MSE). The simulation and successful implementation of MPC in this novel application proves the advantages of such a type of controller when compared to feedback controllers.

This paper is organized as follows: Section II describes the kinematic and dynamic modeling of the ROV. Predictive control with penalty costs is introduced in Section III. Section IV introduces the calculation of the model parameters. Section V demonstrates the simulation and validation of the ROV underwater performance using a Linear Segment with

A. Molero is with the Department of Exploration and Production at PDVSA INTEVEP, Los Teques, Venezuela (moleroaj@pdvsa.com)

R. Dunia is with the Department of Chemical Engineering at The University of Texas, Austin, TX 78712, USA (rdunia@che.utexas.edu)

J. Cappelletto and G. Fernandez are with the Department of Electronics and Circuits at Universidad Simon Bolivar, Caracas, Venezuela (cappelletto,gfernandez @usb.ve)

Parabolic Blend (LSPB) trajectory. Finally, conclusions and future work are provided in Section VI.

II. Modeling of Underwater Vehicles

Modeling permits to simulate the effect of the control actions on the position and velocity of the ROV. The final goal is to predict the optimal control action to apply along a tracking trajectory that the vehicle is expected to follow. These models are based on dragging and gravitational physical laws in a three dimensional space, similar to those obtained for flight vehicles. Nevertheless, traveling across a dense fluid with appreciable buoyancy requires more engine power and velocity than air traveling. Such conditions also allow a better use of all six Degrees of Freedom (DOF) of a rigid object.

Kinematic and dynamic laws provide the mathematical expressions necessary to relate the vector of forces $[X \quad Y \quad Z]^T$ and torques $[K \quad M \quad N]^T$ along the spatial coordinates $[x \quad y \quad z]^T$. This nomenclature is widely used in the published literature of marine vehicles [15] and is illustrated in figure 2. The position and velocity of the ROV are defined by the position of a reference point in the ROV rigid body and its translational movement, respectively. The rotational movements are determined by the rotational angles and their rate of change over time. The following sections provide a detailed description of the first principle equations considered for the kinematic and dynamic modeling of the ROV.

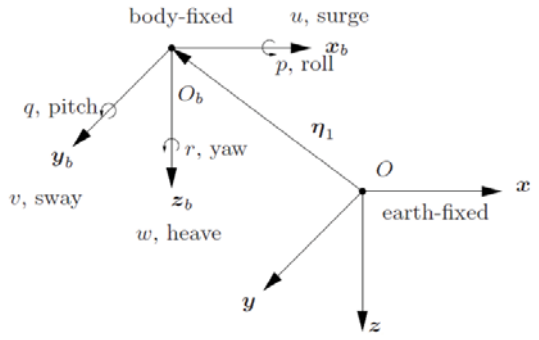

Fig. 2. Body and earth fixed reference frames [16].

A. Kinematics

The motion of underwater vehicles in six DOF is described from two coordinate frames as shown in figure 2. The moving coordinate frame $x_b y_b z_b$ is fixed to the vehicle and is called Body-fixed Reference Frame (BRF). The subindex b denotes the origin of the BRF, and is usually chosen to match the center of gravity of the vehicle, CG.

It is suggested that for underwater vehicles, the BRF axis coincide with the principal axes of inertia, usually named as longitudinal, transverse and normal axis, and denoted by x_b, y_b and z_b, respectively. The earth fixed reference frame is considered as the inertial frame. Based on this nomenclature, the general movement of an underwater vehicle with six DOF can be described by

- The position (η_1) and orientation (η_2) vectors, with coordinates in the inertial reference system fixed on the ground

$$\eta_1 = \begin{bmatrix} x & y & z \end{bmatrix}^T \quad , \quad \eta_2 = \begin{bmatrix} \phi & \theta & \psi \end{bmatrix}^T .$$

For convenience these vectors can be concatenated to form,

$$\eta = \begin{bmatrix} \eta_1^T & \eta_2^T \end{bmatrix}^T .$$

Notice that η provides a snapshot of the rigid vehicle with no reference of moving direction.
- The translation velocity (ν_1) and angular velocity vectors (ν_2) in BRF,

$$\nu_1 = \begin{bmatrix} u & v & w \end{bmatrix}^T \quad , \quad \nu_2 = \begin{bmatrix} p & q & r \end{bmatrix}^T$$

which are also concatenated to form

$$\nu = \begin{bmatrix} \nu_1^T & \nu_2^T \end{bmatrix}^T$$

and represents the velocity vector.
- The force (τ_1) and torque (τ_2) vectors

$$\tau_1 = \begin{bmatrix} X & Y & Z \end{bmatrix}^T \quad , \quad \tau_2 = \begin{bmatrix} K & M & N \end{bmatrix}^T$$

which are also concatenated to form the control action vector, τ

$$\tau = \begin{bmatrix} \tau_1^T, & \tau_2^T \end{bmatrix}^T$$

where τ is manipulated by the controller.

Finally, the vectors η and ν are related by the velocity transformation across the reference system,

$$\dot{\eta} = J(\eta)\,\nu \tag{1}$$

where

$$J(\eta) = \begin{bmatrix} J_1(\eta_2) & \mathbf{0} \\ \mathbf{0} & J_2(\eta_2) \end{bmatrix} \tag{2}$$

and the matrices $J_1(\eta_2)$, $J_2(\eta_2)$ represent the linear and angular velocity transformations, respectively.

B. Dynamics

The following nonlinear dynamics governs the behavior of the ROV,

$$M\dot{\nu} + C(\nu)\,\nu + D(\nu)\,\nu + g(\eta) = \tau, \tag{3}$$

where

- $M \quad \triangleq$ is the inertia matrix, which includes the water mass effect.
- $C(\nu) \triangleq$ is the Coriolis and centripetal matrix with the water mass effects.
- $D(\nu) \triangleq$ is the hydrodynamic damping matrix.
- $g(\eta) \quad \triangleq$ is the vector of forces and moments due to gravity and buoyancy (hydrostatic restoring forces).

The physical meaning of such matrices can be found in [15], [16], where

$$M = M_{RB} + M_A, \tag{4}$$

M_{RB} and M_A are the associated inertia matrices of the ROV and added (water) mass of the PoseiBoT. Their

calculation is based on the ROV symmetrical planes. In a similar manner,

$$C(\nu) = C_{RB}(\nu) + C_A(\nu), \tag{5}$$

where $C_{RB}(\nu)$ and $C_A(\nu)$ are the associated matrices of the Coriolis-centripetal terms of the ROV and added mass, respectively.

The hydrodynamic damping of the ROV can be highly nonlinear and coupled. Nonetheless, an assumption of vehicle independent movement is here considered to neglect high damping coefficients. This assumption results in a matrix structure $D(\nu)$ with linear and quadratic damping coefficients in the main diagonal. The procedure for estimating the theoretical and real values for the hydrodynamic coefficients can be found in [17], [18], [19], [20], [21]. Under low speed considerations and well controlled conditions, the linear and quadratic damping hydrodynamic coefficients are invariant [15] and can be also neglected. Restorative forces and moments are directly described through the gravitational and buoyancy forces.

III. Model Predictive Control

The classic problem of the predictive control [9], [10], lays in minimizing the cost function:

$$J = J_y + J_u + J_{\Delta u}, \tag{6}$$

where each term is explained as follows:

- J_y is the cost function associated with output errors, based on the difference of the controlled variables (outputs) and the reference variables (set-points) along the prediction horizon N_P [12], [9], [10]:

$$J_y(k|k) = \frac{1}{2}\sum_{i=1}^{N_P} \|\hat{\mathbf{y}}(k+i|k) - \mathbf{r}_y(k+i|k)\|_{\mathbb{Q}}^2 \tag{7}$$

  where k is the current sample, $\hat{\mathbf{y}}(k+i|k)$ is the predicted output vector, $\mathbf{r}_y(k+i|k)$ s the expected value of the reference output/set-point evaluating i samples in the future, and $\mathbb{Q}$ is a positive semi-definite matrix of weights, that allows one to penalize the output errors $\mathbf{r}_y - \hat{\mathbf{y}}$. The notation $\|A\|_B^2$ means$\|A\|_B^2 = A^T B\, A$.
- J_u is the cost function associated to the input errors, based on the differences between the action of the control (inputs) and its reference/set-point along the control horizon N_C [12], [9], [10]:

$$J_u(k|k) = \frac{1}{2}\sum_{i=1}^{N_C} \|\mathbf{u}(k+i|k) - \mathbf{r}_u(k+i|k)\|_{\mathbb{N}}^2 \tag{8}$$

  where $\mathbf{u}(k+i|k)$ is the input vector calculated and evaluated i times in the future, $\mathbf{r}_u(k+i|k)$ is the expected input value evaluated i times in the future, and $\mathbb{N}$ is a positive semi-definite matrix of weights, that allows one to penalize the output errors $\mathbf{r}_u - \mathbf{u}$. The term J_u is many times ignored in the cost function [9].
- $J_{\Delta u}$ is the cost function associated to the control action, based on the change in the control action (input movement) along the horizon control N_C [12], [9], [10]:

$$J_{\Delta u}(k|k) = \frac{1}{2}\sum_{i=0}^{N_C-1} \|\Delta\mathbf{u}(k+i|k)\|_{\mathbb{R}}^2 \tag{9}$$

  where $\Delta\mathbf{u}(k+i|k)$ is the change in the control action evaluated i times in the future and $\mathbb{R}$ is a positive definite matrix of weights, that allows to penalize the control action.

The minimization of the cost function J is subject to the following linear constraints,

$$E\begin{bmatrix} \Delta\mathbf{U}(k) \\ 1 \end{bmatrix} \le 0 \quad , \quad F\begin{bmatrix} \mathbf{U}(k) \\ 1 \end{bmatrix} \le 0$$

$$G\begin{bmatrix} \mathbf{Y}(k) \\ 1 \end{bmatrix} \le 0 \tag{10}$$

where $\mathbf{U}(k) = \begin{bmatrix}\hat{u}(k|k)^T & \dots & \hat{u}(k+N_C-1|k)^T\end{bmatrix}^T$. $\hat{u}(k|k)$ is equal to $u(k)$. Similar expressions represent the linear constraints for $\Delta\mathbf{U}(k)$ and $\mathbf{Y}(k)$.

Solving the quadratic programming problem does not guarantee a deterministic, real-time implementation of the controller. Nevertheless, constraints based on barrier function penalties are adjoined to the cost function and permit the deterministic execution of the predictive controller given the response delay required by the ROV (to the controller). This is desirable for systems with fast dynamic responses, like the one in study. The penalty associated to the constraint j is given by the following expression [12]:

$$\mathbf{B}_j(k) = B(l_j, p_j, t_j, z_j(k)), \tag{11}$$

where B is a scalar function with constant parameters l, p and t while z is a time dependent variable. These parameters and the scalar function are best described in [12]. The penalty constraint term is represented by the sum of all possible penalties defined in the control problem. Therefore, the cost function J provided in equation (6) is adjusted to take into account M penalty functions, which express all possible constraints defined by the system in study,

$$J_C = J + \sum_{j=1}^{M}\mathbf{B}_j = J_y + J_u + J_{\Delta u} + \sum_{j=1}^{M}\mathbf{B}_j, \tag{12}$$

where J_C is the objective function with the adjoined constraints and B_j is the accumulative penalty for the j^{th} constraint along the prediction horizon

$$\mathbf{B}_j = \sum_{j=1}^{N_P} B_j(k+i). \tag{13}$$

Quadratic-type penalties are used to simplify the calculation of $\Delta\mathbf{u}$. The implementation of the predictive controller requires the linearization of the model obtained in Section II, which is omitted in this publication. The deployment of the predictive controller is depicted in figure 3.

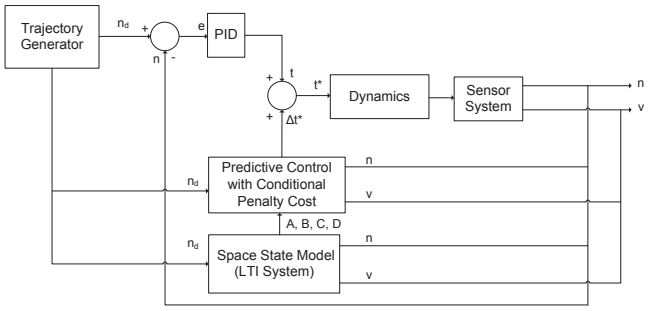

Fig. 3. Predictive control scheme implemented in this application. The main subsystems required for this application were: trajectory generator, model linearizer and predictive controller.

IV. Model Parameters

The modeling of PoseiBoT is characterized by each component piece with its respective mass, the reference system centered at the underwater vehicle's CG, and a coherent orientation. Figure 4 demonstrates a CAD representation of PoseiBot, which provides a useful insight of each control action effect. Table I provides the calculated distance from the robot's CG to the CG of the thrusters/motors,

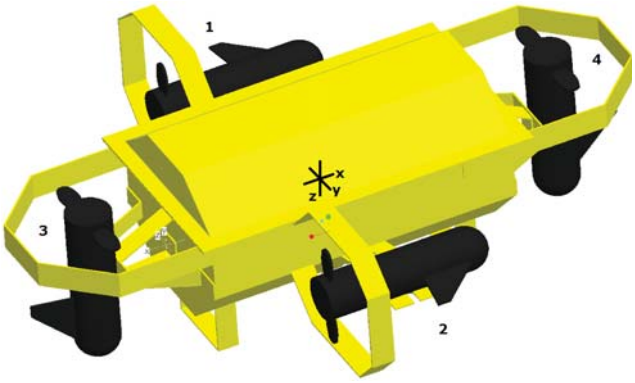

Fig. 4. Three dimensional CAD made for PoseiBoT. Notice the location, translation direction and thrusters enumeration.

TABLE I
Distance [m] between PoseiBoT CG and the different thrusters CG.

Thruster	x (m)	y (m)	z (m)
T1	-0.0288	-0.3126	0.0016
T2	0.0197	0.3339	-0.0061
T3	-0.4673	0.0373	0.0579
T4	0.4621	-0.0381	0.0471

The inertia tensor for the reference system x,y,z is represented by the following matrix:

$$I_G = \begin{bmatrix} I_x & -I_{xy} & -I_{xz} \\ -I_{xy} & I_y & -I_{yz} \\ -I_{xz} & -I_{yz} & I_z \end{bmatrix}.$$

PoseiBoT's mass is about $85\ Kg$. Because only four DOF are used in this system instead of six (one per each thruster), a mapping between the thrusters and the force-torque vector τ is necessary. Such a mapping is defined by the constant matrix L, where $\tau = LT$ and

$$T = \begin{bmatrix} T1 & T2 & T3 & T4 \end{bmatrix}^T.$$

The Appendix provides the numerical values obtained for I_G, L and the linearization of the under water vehicle model when only translation in the x and z directions are considered. The state vector for the linearized model is defined in terms of deviation variables,

$$\mathbf{x} = \begin{bmatrix} u - u_0 & w - w_0 & x - x_0 & z - z_0 \end{bmatrix}^T,$$

and C_l is the identity matrix.

$$\mathbf{y} = \mathbf{x} = \begin{bmatrix} u - u_0 & w - w_0 & x - x_0 & z - z_0 \end{bmatrix}^T,$$

where $\begin{pmatrix} x_0, & z_0 \end{pmatrix}^T$ are given by the desired trajectories and $\begin{pmatrix} u_0, & w_0 \end{pmatrix}^T$ are calculated using equation (1). The vector $\begin{pmatrix} u, w, x, z \end{pmatrix}^T$ is measured by the ROV instrumentation. Finally, the LTI model is given by

$$\dot{\mathbf{x}} = A_r\mathbf{x} + B_r\mathbf{u}$$

$$\mathbf{y} = C_l\mathbf{x}$$

where $\mathbf{u} = \Delta\tau = \tau - \tau_\mathbf{0}$, and the matrices A_r, B_r are given in the Appendix.

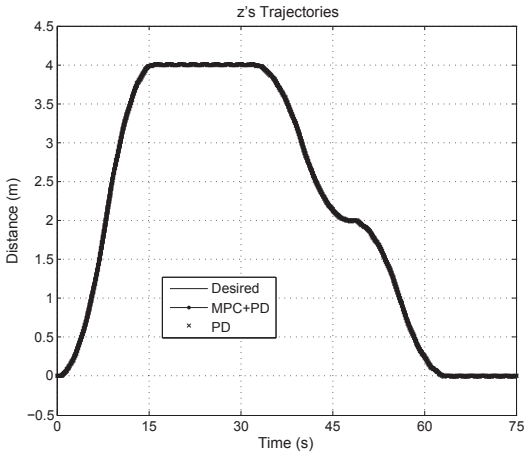

Fig. 5. Trajectory profile in the z coordinate. The ROV trajectory overlaps the desired trajectory in the simulation framework.

V. Results

A LSPB was traced along the z axis to test the MPC controller. No tests were performed along the x and y axis because the current platform doesn't provide instrumentation for such coordinates. Therefore, the variables $Pitch$, $Roll$ and Yaw were set to zero. Figure 5 illustrates the reference-desired trajectory, MPC + PD trajectory and PD performance trajectory in z. Figure 6 is obtained by zooming into an area of interest, which demonstrates that the system performs better with both a predictive controller and a proportional-derivative controller than it does with a proportional-derivative controller alone. Such a qualitative

result is quantified in Table III, which shows the RMS values required for the thrusters.

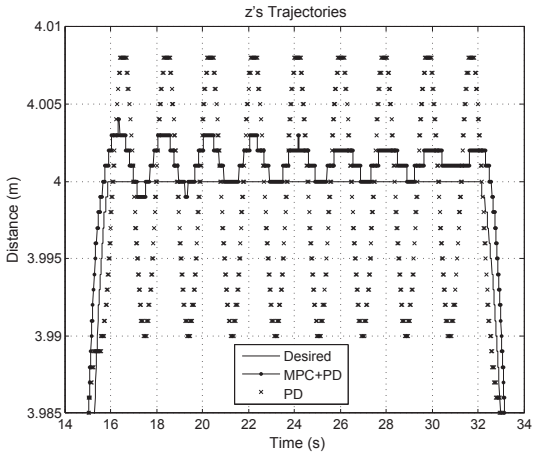

Fig. 6. Detailed response from figure 5 for the time frame given by $14 \leq t \leq 34$.

TABLE II
CONTROLLER PERFORMANCE COMPARISON BASED ON MSE VALUES (SIMULATION).

Controller	Trajectory	MSE (m)
PD	z	0.0066
MPC+PD	z	**0.0040**

TABLE III
RMS VALUES OF THE REQUIRED THRUSTERS FORCES (SIMULATION)

Thruster	RMS value using PD (N)	RMS value using MPC+PD (N)
T3-T4	4.1139	**0.9578**

As observed in figures 5 and 6, and tables II and III the amount of force required by the thrusters to perform the desired trajectory using predictive control is significantly less than it was when using the proportional-derivative control. It was practically possible to reduce the tracking error by 40% with a 76% reduction in the stringent control signal. This shows that the predictive control described in [12] offers excellent performance.

The z position is estimated through the use of four pressure sensors located on the underside of PoseiBoT. To achieve better accuracy in the z measurement, a median filter was used for the pressure sensors, and the intermediate outputs of this filter were averaged. The depth sensor is calibrated for a maximum pressure equal at 5 m (depth maximum of the pool used).

The following factors were considered during testing:

- Dynamics of the submarine -fast- vs. controller -slow-
- Slow implementation of controllers
- Communication errors between the microprocessor and pressure sensors, yielding poor estimate of the distance in z (depth).

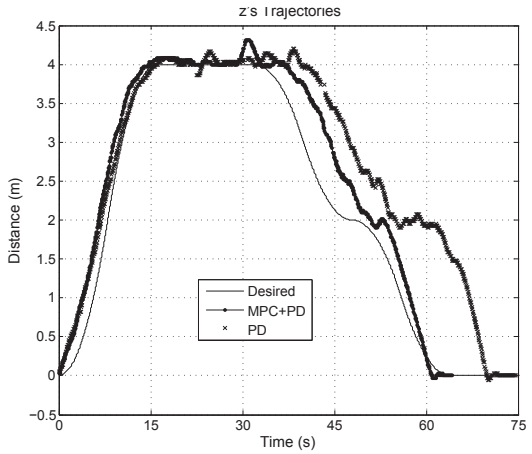

Fig. 7. Trajectory profile in the z coordinate: desired and performed trajectories followed by PoseiBoT using the MPC+PD and PD controllers. The MPC controller acts promptly to follow the desired trajectory.

A PI controller was implemented to eliminate a small inclination in the Pitch of the ROV. This controller was implemented outside the control scheme described in figure 3 and its output was added to the thruster forces T_3 and T_4. Figure 7 shows the results obtained by testing the model in closed loop with a PD controller and using the predictive controller developed in section III, in addition to the desired trajectory. As it was noted, the MPC controller + PD offers better results, because it follows the trajectory in the desired time, which does not happen using the PD controller. This proves that the predictive controller can follow trajectories that are relatively fast, and also a better tracking.

Table IV shows the MSE for the trajectories performed by the PoseiBoT. In this case the predictive controller offers better performance compared to the PD along the defined trajectory in z.

TABLE IV
MSE PERFORMANCE COMPARISON FOR THE DIFFERENT CONTROLLERS (IMPLEMENTATION)

Controller	MSE z (m)	MSE $Pitch$ (°)
PD	0.4869	**0.1360**
MPC+PD	**0.0969**	0.1367

Table V shows the RMS values of the forces required by the thrusters $T3$ and $T4$, where the MPC + PD controller achieved the desired trajectory. The PD did not perform at the specified time, and it a less effective inclination control with greater control effort. The results show that MPC can reduce the tracking error (MSE) by 80% while reducing the control action (RMS) by 13.91%.

TABLE V
RMS VALUES OF THE REQUIRED THRUSTERS FORCES. (VALIDATION)

Thruster	RMS using the PD controller	RMS using the MPC+ PD controller
T3	83.3950	**72.3631**
T4	88.2674	**75.3926**

VI. Conclusions

This work demonstrates that MPC provides better tracking with less control effort than classical feedback controllers. The results show that MPC can reduce the tracking error by 40% with 76% reduction in the control action compared to a PD controller. The approximations made during the vehicle model development provides an acceptable prediction for the controller. Minor difference obtained between the simulations and validation tests are due to added mass coefficient approximations, an inacurate linearized model, estimation of the elements configured in the CAD model towards property calculations and the inertia tensor matrix approximation. It is important to determine and validate all the parameters of the model in a rigorous way, and to test them accordingly. For this reason the use of system identification techniques are expected to assist developing future improvements of this application.

Appendix

The inertia tensor matrix is given by $[kg.m^2]$,

$$I_G = \begin{bmatrix} 2.835 & -1.81 \times 10^{-3} & -2.47 \times 10^{-1} \\ -1.81 \times 10^{-3} & 8.122 & -3.16 \times 10^{-3} \\ -2.47 \times 10^{-1} & -3.16 \times 10^{-3} & 6.117 \end{bmatrix}$$

while the mapping matrix between the forces-torques and the trusters in given by

$$L = \begin{bmatrix} 1 & 1 & 0 & 0 \\ 0 & 0 & 0 & 0 \\ 0 & 0 & 1 & 1 \\ 0 & 0 & 0.0373 & -0.0381 \\ 0.0016 & -0.0061 & 0.4673 & -0.4621 \\ 0.3126 & -0.3339 & 0 & 0 \end{bmatrix}$$

The matrices obtained from the linearized model are given by:

$$\begin{aligned} A_r &= \begin{bmatrix} -M_r^{-1}\left[C_r + D_r\right] & -M_r^{-1} G_r \\ J_r & 0_{2\times 2} \end{bmatrix} \\ B_r &= \begin{bmatrix} M_r^{-1} \\ 0_{2\times 2} \end{bmatrix} \end{aligned}$$

where

$$\begin{aligned} M_r &= \begin{bmatrix} m - X_{\dot{u}} & 0 \\ 0 & m - Z_{\dot{w}} \end{bmatrix} \\ &= \begin{bmatrix} 113.0572 & 0 \\ 0 & 136.5692 \end{bmatrix} \\ C_r &= G_r = 0_{2\times 2} \\ J_r &= -D_r = I_{2\times 2} \end{aligned}$$

Substitution into the system matrices A_r and B_r gives

$$\begin{aligned} A_r &= \begin{bmatrix} 0.0088 & 0 & 0 & 0 \\ 0 & 0.0073 & 0 & 0 \\ 1 & 0 & 0 & 0 \\ 0 & 1 & 0 & 0 \end{bmatrix} \\ B_r &= \begin{bmatrix} 0.0088 & 0 \\ 0 & 0.0073 \\ 0 & 0 \\ 0 & 0 \end{bmatrix} \end{aligned}$$

which provides a controllable pair (A_r, B_r).

References

[1] Hudson, I.R., Jones, D.O.B. and Wigham, B.D., "A review of the uses of work-class ROVs for the benefits of science: lessons learned from the SERPENT project", *Underwater Technology*, 2005.

[2] Inoue, T., Osawa, H., Yoshida, H., Tahara, J., Ishibashi, S., Ito, K., Watanabe, Y., Sawa, T. and Hyakudome T., "Sea Trial Results of ROV ABISMO for Deep Sea Inspection and Sampling", *ASME 2008 27th International Conference on Offshore Mechanics and Arctic Engineering (OMAE2008)*, 2008.

[3] Jordan, M.A. and Bustamante, J.L., "Guidance of Underwater Vehicles With Cable Tug Perturbations Under Fixed and Adaptive Control Systems", *IEEE Journal of Oceanic Engineering*, 2008.

[4] Caccia, M. and Veruggio, G., "Guidance and control of a reconfigurable unmanned underwater vehicle", *Control Engineering Practice*, 2000.

[5] Gomes, R.M.F., De Sousa, J.B. and Pereira, F.L., "Integrated maneuver and control design for ROV operations", *OCEANS MTS/IEEE: Conference on Celebrating the Past - Teaming Toward the Future*, 2003.

[6] Guo, J., Chiu, F C., Cheng, S W. and Pan J W., "Robust trajectory control of a remotely operated vehicle for underwater inspection tasks", *3rd International Workshop on Scientific Use Submarine Cables and Related Technologies*, 2003.

[7] Whitcomb, L.L., Howland, J.C., Smallwood, D.A., Yoerger, D.R. and Thiel, T.E., "A new control system for the next generation of US and UK deep submergence oceanographic ROVs", *IFAC Workshop on Guidance and Control of Underwater Vehicles*, 2003.

[8] Soylu, S., Buckham, B.J. and Podhorodeski, R.P., "Robust control of underwater vehicles with fault-tolerant infinity-norm thruster force allocation", *2007 OCEANS Conference*, 2007.

[9] Maciejowski, J.M., "Predictive Control with Constraints", Prentice Hall, 2000.

[10] Camacho, E. and Bordons, C. "Model Predictive Control", Springer-Verlag, 1999.

[11] Qin, S.J. and Badgwell, T.A., "A survey of industrial model predictive control technology", *Control Engineering Practice*, 2003.

[12] Dunia, R. and Fernandez, G., "MPC with Conditional Penalty Cost", IECON 2009 - *The 35th Annual Conference of the IEEE Industrial Electronics Society*, 2009.

[13] Spong, M., Hutchinson, S. and Vidyasagar, M., "Robot Modeling and Control". John Wiley & Sons, 2006

[14] Siciliano, B., Sciavicco, L., Villani, L. and Oriolo, G., "Robotics: Modelling, Planning and Control", Springer, 2009.

[15] Foseen, T., "Guidance and Control of Ocean Vehicles". John Wiley & Sons Ltd, 1994.

[16] Antonelli, G., "Underwater Robots: Motion and Force Control of Vehicle-Manipulator Systems". Springer - Advanced Robotics, 2006.

[17] Gonzalez, L.A. "Design, Modelling and Control of an Autonomous Underwater Vehicle", University of Western Australia, 2004.

[18] Bilo, D. and Nachtigall, W., "A Simple Method to Determine Drag Coefficients in Aquatic Animals". *Journal of Experimental Biology*, 1980.

[19] Ridao, P., Batlle, J. and Carreras, M., "Model Identification of a Low-Speed UUV with on-board sensors". *IFAC conference CAMS'2001, Control Applications in Marine Systems*, 2001.

[20] Ridao, P., Tiano, A., El-Fakdi, A., Carreras, M. and Zirilli, A., "On the identification of non-linear models of unmanned Underwater Vehicle", *Control Engineering Practice*, 2004.

[21] Rentschler, M., "Dynamic Simulation Modeling and Control of the Odyssey III Autonomous Underwater Vehicle", Massachusetts Institute of Technology, 2003.

[22] Cabrera, M.E and Ruella, C. "Diseno y construccion de un sistema de instrumentacion y control para la plataforma robotica PoseiBoT". Universidad Simon Bolivar, 2008.